Organic & Biomolecular Chemistry

PAPER

View Article Online
View Journal | View Issue

Cite this: *Org. Biomol. Chem.*, 2014, **12**, 5645

Selective recognition of anionic cell membranes using targeted liposomes coated with zinc(II)-bis(dipicolylamine) affinity units†

Serhan Turkyilmaz,[a,b] Douglas R. Rice,[a] Rachael Palumbo[a] and Bradley D. Smith*[a]

Received 5th May 2014,
Accepted 18th June 2014

DOI: 10.1039/c4ob00924j

www.rsc.org/obc

Zinc(II)-bis(dipicolylamine) (Zn_2BDPA) coated liposomes are shown to have high recognition selectivity towards vesicle and cell membranes with anionic surfaces. Robust synthetic methods were developed to produce Zn_2BDPA-PEG-lipid conjugates with varying PEG linker chain length. One conjugate (Zn_2BDPA-PEG_{2000}-DSPE) was used in liposome formulations doped with the lipophilic near-infrared fluorophore DiR. Fluorescence cell microscopy studies demonstrated that the multivalent liposomes selectively and efficiently target bacteria in the presence of healthy mammalian cells and cause bacterial cell agglutination. The liposomes also exhibited selective staining of the surfaces of dead or dying human cancer cells that had been treated with a chemotherapeutic agent.

Introduction

Zinc(II)-bis(dipicolylamine) (Zn_2BDPA) coordination complexes are known to associate with phosphate polyanions in aqueous solution (Fig. 1A) and they have been developed for various supramolecular applications such as optical chemosensing, biomolecule labeling and catalytic hydrolysis.[1–21] We have contributed to this effort by demonstrating that Zn_2BDPA complexes have selective affinity for anionic cell membrane surfaces over the near-neutral membrane surfaces of healthy mammalian cells.[22–28] This discovery has led to molecular imaging probes that can target two types of anionic cell systems with high biomedical significance, namely, bacterial cells and dead/dying mammalian cells. With bacterial cells, the surrounding envelope is anionic because it contains phosphorylated amphiphiles such as phosphatidylglycerol or lipotechoic acid in the case of Gram-positive bacteria, or lipid A in the case of Gram-negative bacteria. With dead/dying mammalian cells, the outer membrane surface becomes anionic due to the exposure of phosphatidylserine during the cell death process. We have shown that fluorescent Zn_2BDPA probes can selectively stain these anionic cells even when they are within highly complex and heterogeneous biological environments such as cell culture and living animals.[22–28]

Recently, we prepared and evaluated multivalent Zn_2BDPA molecular probes that were equipped with four or more covalently attached Zn_2BDPA targeting units and observed high selectivity for anionic membranes.[29–31] Fluorescent versions of these multivalent Zn_2BDPA probes were found to be effective optical imaging agents in cell culture and animal models of bacterial infection or cell death. A notable finding with the bacterial studies was the strong propensity of multivalent Zn_2BDPA probes to selectively cross-link and agglutinate bacterial cells. The multivalent Zn_2BDPA probes were not bactericidal, but the agglutination effect was universal regardless of Gram-type or cell morphology. These results suggest that multivalent Zn_2BDPA molecular probes have promise as selective, broad spectrum bacterial agglutination agents for infection imaging and diagnostics. Similarly, they may also be incorporated into imaging and theranostic strategies that target mammalian cell death. For example, a hypothetical cancer treatment strategy might employ a multifunctional drug delivery vehicle to target the sites of endogenous cell death within a tumor. If the tumor is responsive to the delivered drug, more cell death occurs which, in principle, should amplify the drug delivery process during a subsequent treatment.[32,33]

A necessary requirement for each of these potential imaging and theranostic applications is the construction of effective multivalent Zn_2BDPA imaging probes and drug delivery vehicles. We were attracted to liposomes as a biocompatible nanoparticle platform whose pharmacokinetic properties can be optimized by systematic modification of the amphiphilic building blocks. The ability of non-targeted stealth liposomes to exploit the enhanced permeation retention (EPR)

[a]*Department of Chemistry and Biochemistry, 236 Nieuwland Science HallUniversity of Notre Dame, Notre Dame, IN 46556, USA. E-mail: smith.115@nd.edu*
[b]*Faculty of Pharmacy, Department of Pharmaceutical Chemistry, Istanbul University, 34116 Beyazit, Istanbul, Turkey*

† Electronic supplementary information (ESI) available: Spectral data, liposome characterization and cell toxicity data. See DOI: 10.1039/c4ob00924j

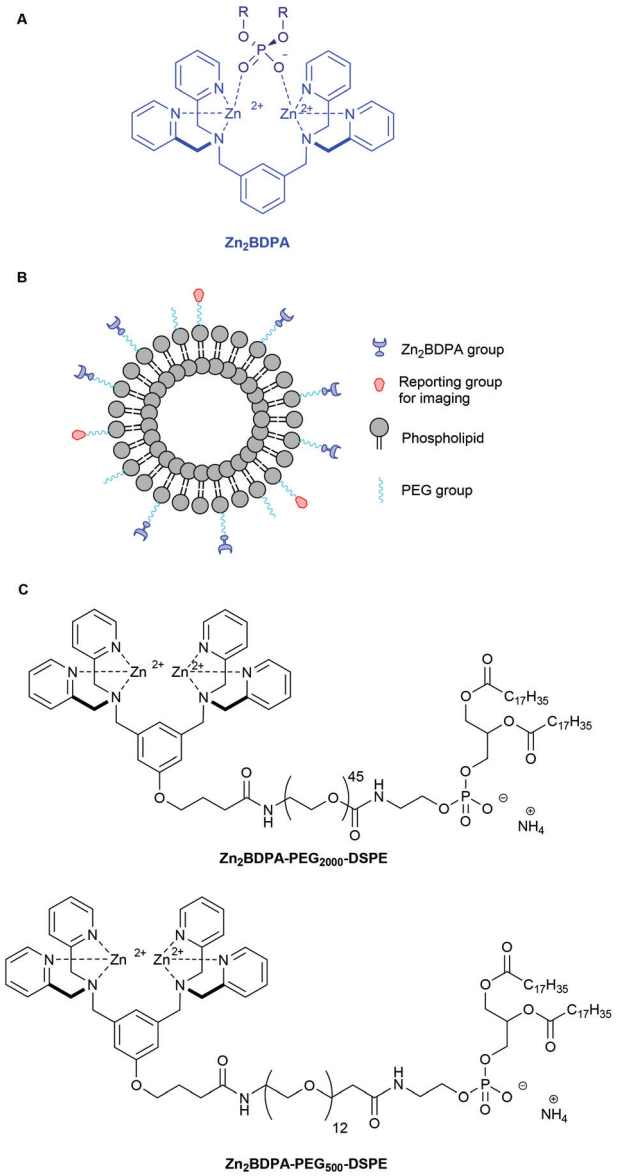

Fig. 1 Association of a Zn_2BDPA coordination complex with a phosphodiester (A), schematic picture of a Zn_2BDPA coated liposome with PEG and Zn_2BDPA groups on the inner leaflet omitted for clarity (B), structures of Zn_2BDPA-lipid conjugates used in this study (C).

effect and accumulate inside tumors is well known as one of the pioneering success stories of nanomedicine.[34,35] In related fashion, stealth liposomes are known to collect in sites of bacterial infection within living subjects.[36] In both of these cases, the liposome accumulation process is passive and does not involve direct molecular targeting. This present report, on the targeting ability of liposomes that are coated with multiple Zn_2BDPA affinity units, is the first step in a process to develop targeted liposome systems that enhance the passive accumulation effects described above. There is a large and growing body of literature on the topic of targeted liposomes; that is, liposomes coated with targeting ligands having selective affinity for receptors or biomarkers of disease. Although the concept of targeted liposomes has alluring features, it also includes molecular design challenges that must simultaneously address conflicting requirements.[37–42] Most notable is the need to coat the liposome surface with polymeric structures (*e.g.*, PEG chains) that inhibit recognition and premature clearance of the liposomes by the reticuloendothelial system (RES). One potential solution is to attach the targeting ligands to the ends of the polymeric chains, but the current literature on this strategy does not make it clear if the targeting ligands will still be available for receptor binding, or if they will trigger undesired recognition by the RES. There is also the nontrivial synthetic chemistry challenge of fabricating the targeted liposomes. The most common approach is to append the targeting ligands to the ends of commercially available polyethyleneglycol-phospholipid conjugates such as PEG_{2000}-DSPE. There are two limiting strategies. One is to react the targeting ligand with preformed liposomes containing a suitably reactive PEG_{2000}-DSPE. The other approach is to first synthesize the functionalized PEG_{2000}-DSPE conjugate and then assemble the liposomes. The latter method provides more opportunity to validate compositional purity of the liposome components, but there are still molecule characterization challenges due to polydispersity of the PEG chains in most commercial supplies of the starting materials. We believe that studies of targeted liposomes are best conducted using molecular building blocks with well-defined chemical structures and high compositional purity.

Here, we describe the preparation of targeted liposomes that are coated with multiple Zn_2BDPA affinity units through the incorporation of a small fraction of amphiphilic Zn_2BDPA-PEG-DSPE conjugates in the bilayer membranes (Fig. 1B). Specifically, we describe the synthesis of two conjugates, Zn_2BDPA-PEG_{2000}-DSPE and Zn_2BDPA-PEG_{500}-DSPE (Fig. 1C) and the *in vitro* molecular recognition properties of liposomes that incorporate these conjugates. We find that Zn_2BDPA coated liposomes are able to rapidly cross-link a second population of anionic liposomes. Furthermore, we show that Zn_2BDPA coated liposomes can selectively agglutinate bacterial cells in the presence of healthy mammalian cells and also selectively target the surfaces of dead/dying mammalian cancer cells. The results indicate that Zn_2BDPA coated liposomes have great promise for wide range of targeted imaging and drug delivery applications.

Results and discussion

Synthesis and liposome preparation

Our strategy for the construction of Zn_2BDPA-PEG-lipid conjugates was largely determined by the commercial availability of lipids and PEGylated lipids suitable for conjugation. Lipids terminating in amine groups such as DSPE and NH_2-PEG_{2000}-DSPE are commercially available. Furthermore, bis(dipicolylamine) (BDPA) conjugates of these lipids can be prepared through standard amide coupling chemistry. The BDPA carboxylic acid derivative **6**, which would allow the preparation of

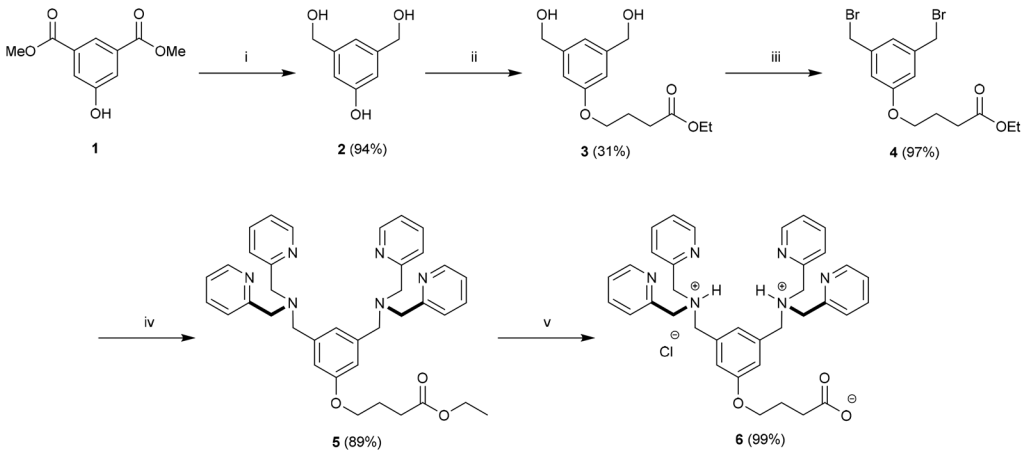

Scheme 1 Preparation of BDPA carboxylic acid **6**. Conditions: (i) $LiAlH_4$, THF, rt, 24 h; (ii) Ethyl 4-bromobutyrate, K_2CO_3, Bu_4NI, 60 °C, 16 h; (iii) Ph_3P, CBr_4, DIPEA, THF, rt, 24 h; (iv) 2,2′-dipicolylamine, K_2CO_3, DMF, rt, 16 h; (v) 2 : 1 : 1 THF–H_2O–MeOH, NaOH, reflux, 2 h.

these conjugates, was synthesized in a fashion similar to a BDPA amine derivative we reported earlier.[43] Accordingly, dimethyl 5-hydroxyisophthalate (**1**) was reduced using $LiAlH_4$ to give 3,5-bis(hydroxymethyl)phenol (**2**) in high yield,[44] which was coupled with ethyl 4-bromobutanoate using K_2CO_3/Bu_4NI in anhydrous DMF to give **3** in 31% yield. Numerous attempts at improving the yield for this alkylation proved fruitless. The diol **3** was efficiently converted to the dibromo derivative **4** using modified Appel conditions.[45] The ligands for zinc were installed by reacting **4** with dipicolylamine using K_2CO_3 in anhydrous DMF to give **5** in good yield. Finally saponification of **5** afforded the desired BDPA carboxylic acid **6** quantitatively (Scheme 1).

With **6** in hand we turned our attention to the preparation of BDPA-PEG_{2000}-DSPE (**7**). A multitude of methods can be considered for the amide bond formation between **6** and H_2N-PEG_{2000}-DSPE.[46] We found that the EDC/DMAP mediated pentafluorophenol (PfpOH) activation of **6** followed by reaction with H_2N-PEG_{2000}-DSPE reliably afforded BDPA conjugate **7** (Scheme 2). Using this method it was possible to prepare tens of milligrams of **7** in one run and purification merely consisted of a relatively simple preparatory TLC procedure. It should be noted that commercially available H_2N-PEG_{2000}-DSPE is a polydisperse mixture of PEG chains with a mean degree of polymerization around 45 and this is reflected in the HRMS spectrum of **7** (ESI). To remove the mass spectral ambiguity regarding the identity of the product and to demonstrate the versatility of the synthetic methods we decided to prepare BDPA-PEG_{500}-DSPE (**10**) from commercially available monodisperse FmocNH-PEG_{500}-propionic acid (**8**). Reaction of PfpOH activated **8** with DSPE proved very sluggish in a wide variety of solvents due to the poor solubility of this phospholipid. This problem was overcome by refluxing the reaction. Removal of the Fmoc group using piperidine and reaction of the resulting H_2N-PEG_{500}-DSPE (**9**) with PfpOH activated **6** afforded the desired conjugate **10** in good yield (Scheme 3). It was possible to purify **10** using a relatively simple preparatory TLC procedure and the spectral data indicated monodispersity.

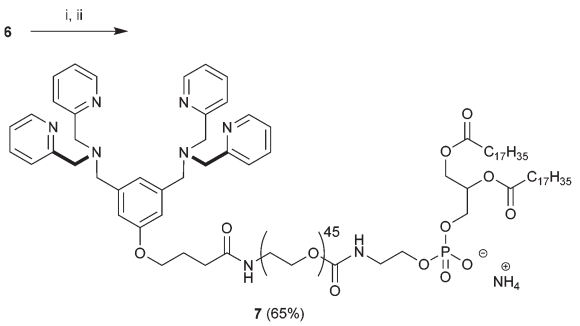

Scheme 2 Preparation of BDPA-PEG_{2000}-DSPE (**7**). Conditions: (i) PfpOH, EDC, DMAP, $CHCl_3$, 0 °C to rt, 16 h followed by (ii) H_2N-PEG_{2000}-DSPE, DIPEA, $CHCl_3$, rt, 24 h.

For cuvette experiments, liposomal dispersions containing 2.5 mol% of the Zn_2BDPA-PEG-DSPE amphiphiles were prepared using the film hydration/extrusion method.[47] Lipid films composed of **7**–cholesterol–POPC or **10**–cholesterol–POPC (2.5 : 30 : 67.5 mol%, 3.32 μmol total lipid) were hydrated using HEPES buffer containing $Zn(NO_3)_2$. The Zn^{2+}/BDPA molar ratio was 10 to ensure rapid and complete formation of the Zn_2BDPA coordination complexes. In the absence of Zn^{2+}, the dispersions were impossible to extrude, presumably due to bilayer self-aggregation caused by the lipophilic nature of the uncomplexed BDPA units. In the presence of Zn^{2+}, the lipid films were readily dispersed into aqueous solution and easy to extrude through polycarbonate membranes with 200 nm diameter pores. Dynamic light scattering (DLS) analysis of the liposomes composed of Zn_2BDPA-PEG_{2000}-DSPE–cholesterol–POPC (2.5 : 30 : 67.5) indicated a monomodal size distribution with diameter = 154 ± 54 nm, PDI = 0.109, and ζ = 4.82 mV. The same analysis of liposomes composed of Zn_2BDPA-PEG_{500}-DSPE–cholesterol–POPC (2.5 : 30 : 67.5) indicated a bimodal size distribution with two diameters = 96 ± 15 nm, and 790 ± 140 nm, PDI = 1.000, and ζ = 4.00 mV. We infer that the larger diameter is due to liposome self-aggregation. Most likely, the shorter PEG chain in the Zn_2BDPA-PEG_{500}-DSPE is

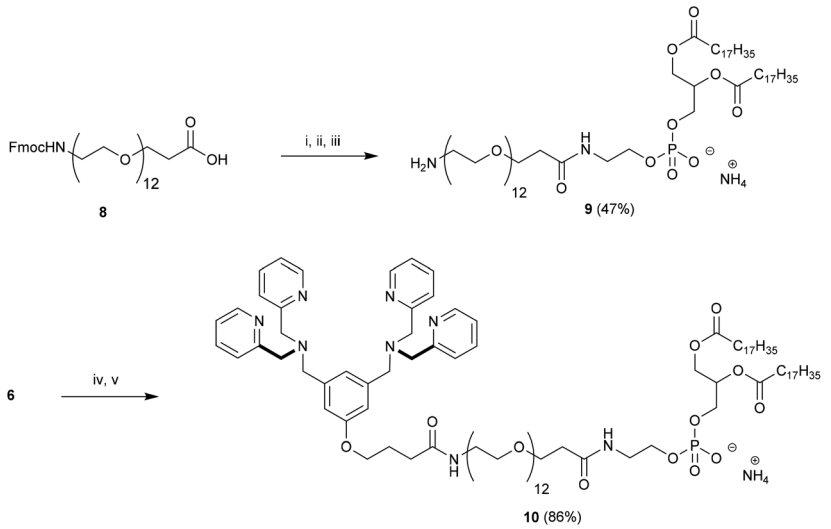

Scheme 3 Preparation of BDPA-PEG_{500}-DSPE (**10**). Conditions: (i) PfpOH, EDC, DMAP, $CHCl_3$, 0 °C to rt, 16 h followed by (ii) DSPE, DIPEA, $CHCl_3$, reflux, 24 h; (iii) piperidine–DMF 2 : 8, rt, 2 h; (iv) PfpOH, EDC, DMAP, $CHCl_3$, 0 °C to rt, 16 h followed by (v) **9**, DIPEA, $CHCl_3$, rt, 24 h.

unable to fully block association of the terminal Zn_2BDPA affinity units with the negatively charged phosphate diester groups on the opposing bilayer surface. Self-aggregation was not observed with the liposomes containing Zn_2BDPA-PEG_{2000}-DSPE, (four times longer PEG chain), therefore, all subsequent studies of Zn_2BDPA coated liposomes used membrane compositions containing this conjugated amphiphile.

The selective affinity of Zn_2BDPA coated liposomes for anionic membranes was vividly demonstrated by conducting experiments that mixed liposomes composed of Zn_2BDPA-PEG_{2000}-DSPE–cholesterol–POPC (2.5 : 30 : 67.5) with target liposomes of various compositions. As shown in Fig. 2, mixing with anionic liposomes composed of POPS–cholesterol–POPC (10 : 30 : 60) resulted in rapid and extensive precipitation. Mixing with anionic liposomes composed of DPPG–cholesterol–POPC (10 : 30 : 60) produced the same outcome (see ESI†). In contrast, mixing with uncharged liposomes composed of cholesterol–POPC (30 : 70) produced no precipitation. Control experiments showed that the anionic liposome systems do not form aggregates when exposed to $Zn(NO_3)_2$ alone, thus confirming that the Zn_2BDPA affinity units are essential for the anionic membrane recognition process. These favorable liposome targeting results encouraged us to conduct cell recognition studies using both human and bacterial cells. The liposomes were doped with a small amount of the near-infrared fluorescent lipophilic dye, DiR, to enable effective visualization using fluorescence microscopy.

Fig. 2 Cross-linking of liposomes containing Zn_2BDPA-PEG_{2000}-DSPE and anionic target liposomes containing POPS. (A) Liposomes composed of Zn_2BDPA-PEG_{2000}-DSPE–cholesterol–POPC (2.5 : 30 : 67.5 mol%, 0.83 μmol total lipid) in zinc-containing HEPES buffer. (B) Liposomes composed of POPS–cholesterol–POPC (10 : 30 : 60 mol%, 0.83 μmol total lipid) in zinc-containing HEPES buffer. (C) Admixture of liposome samples A and B.

Selective bacteria targeting using Zn_2BDPA coated liposomes

The bacterial targeting of Zn_2BDPA coated liposomes was evaluated by conducting imaging experiments using cultures of *E. coli*, *P. aeruginosa*, *S. aureus*, and *K. pneumoniae*. In each case, separate samples of bacteria (~10^8 cells) were treated for 15 min with Zn_2BDPA coated liposomes (Zn_2BDPA-PEG_{2000}-DSPE–DiR–cholesterol–POPC, 2 : 2 : 30 : 66) or untargeted liposomes (DiR–cholesterol–POPC, 2 : 30 : 68). The treated cells were pelleted by microcentrifugation and the tubes were imaged using a CCD camera. As shown in Fig. 3, the fluorescent Zn_2BDPA coated liposomes were located primarily in the bacterial pellet, whereas, the fluorescent untargeted liposomes were primarily in the supernatant above the pellet. After pellet imaging, the bacterial cells were rinsed twice, dispersed into solution by vortexing, and subjected to fluorescence microscopy. Shown in Fig. 4 are typical micrographs of cross-linked bacteria/liposome aggregates. Analogous micrographs of the pelleted bacteria that had been treated with fluorescent untargeted liposomes showed no evidence for bacterial cross-linking (Fig. ESI-6†).

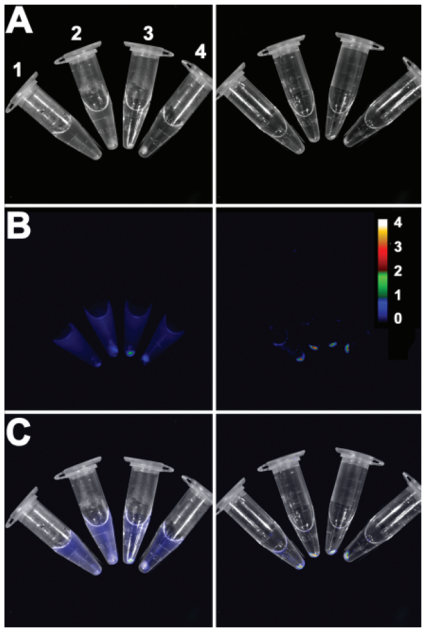

Fig. 3 Four strains of pelleted bacteria after treatment with fluorescent untargeted liposomes (left column) or fluorescent Zn_2BDPA coated liposomes (right column) and imaged using a CCD camera. (A) Brightfield; (B) near-infrared fluorescence; (C) merge. 1 = *E. coli*, 2 = *P. aeruginosa*, 3 = *S. aureus* and 4 = *K. pneumoniae*. Scale bar indicates near-infrared emission intensity for both fluorescence images in row B.

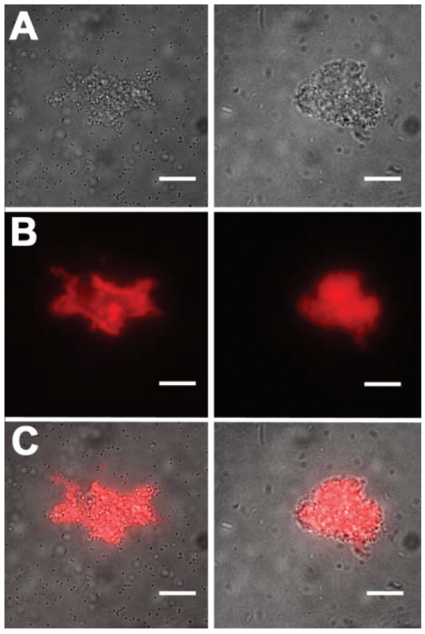

Fig. 4 Representative fluorescence microscopy images of bacteria after treatment with fluorescent Zn_2BDPA coated liposomes. (left column) Gram-positive *S. Aureus* bacteria, (right column) Gram-negative *E. coli*. (Top row) Brightfield image of cross-linked bacteria/liposome aggregate; (Middle row) Near-infrared fluorescence emission from Zn_2BDPA liposomes bound to the bacteria; (Bottom row) Overlay of brightfield and fluorescence images. No fluorescence staining of bacterial cells was observed with fluorescent untargeted liposomes. Scale bar = 30 μm.

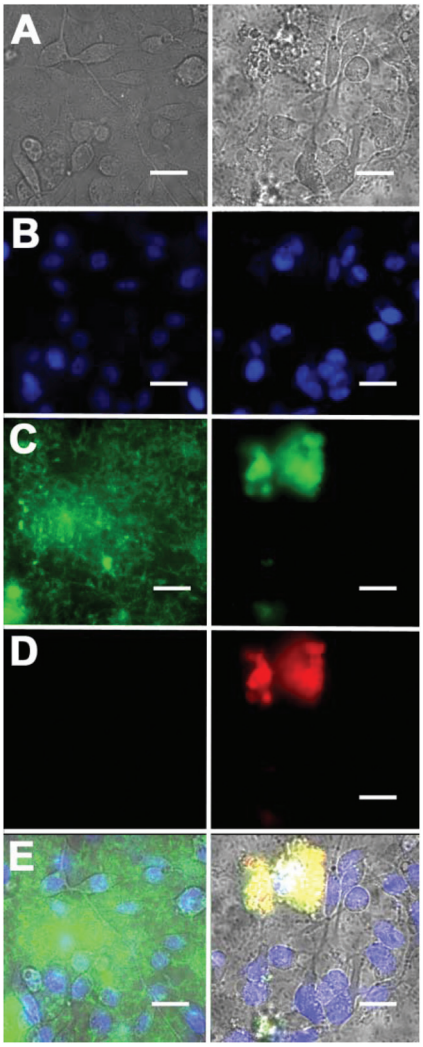

Fig. 5 Fluorescence micrographs of a mixture of DAPI stained MDA-MB-211 human breast cancer cells, GFP-expressing *P. aeruginosa*, and either near-infrared fluorescent untargeted liposomes (left column) or near-infrared fluorescent Zn_2BDPA coated liposomes (right column). (row A) Brightfield images; (row B) Human cell nuclei stained with blue-emitting DAPI; (row C) green-emitting *P. aeruginosa*; (row D) near-infrared fluorescence from Zn_2BDPA coated liposomes; (row E) Overlay of A, B, C and D. Scale bar = 30 μm.

Additional cell microscopy experiments demonstrated the selectivity of the Zn_2BDPA coated liposomes for bacterial cells over healthy mammalian cells. Mixtures of near-infrared fluorescent liposomes (coated with Zn_2BDPA or untargeted), MDA-MB-211 human breast cancer cells and GFP-expressing *P. aeruginosa* bacteria were incubated for 15 min. As shown in Fig. 5, only the mixtures with Zn_2BDPA coated liposomes resulted in bacterial agglutination. Fig. 5C and 5D show strong co-localization of the near-infrared Zn_2BDPA coated liposomes and the green bacterial fluorescence, and no association of the Zn_2BDPA coated liposomes with the mammalian cell surfaces. The untargeted liposomes did not interact with the bacteria which remained widely dispersed across the entire micrograph. These results are consistent with our previous

observations using multivalent molecular probes with four or more covalently attached Zn_2BDPA targeting units, and the independent work of others who have reported that magnetic Zn_2BDPA nanoparticles can be used to separate bacterial cells from mammalian blood cells.[48]

Mammalian cell death targeting using Zn_2BDPA coated liposomes

Standard MTT cell vitality assays showed that the Zn_2BDPA coated liposomes were not toxic to MDA-MB-231 human breast cancer cells (Fig. ESI-7†). Furthermore, fluorescence microscopy studies showed that fluorescently labeled Zn_2BDPA coated liposomes did not stain healthy MDA-MB-231 cells, but they did stain dead and dying cells that had been treated with a cytotoxic agent. Specifically, MDA-MB-211 cells were incubated with etoposide (10 μM) followed by fluorescent liposomes and PSVue480, a commercially available Zn_2BDPA-fluorescein molecular conjugate that has been validated as a green-emitting fluorescent probe that targets exposed PS on the exterior of dead and dying cells. As shown in Fig. 6, the near-infrared Zn_2BDPA coated liposomes co-localized with PSVue480. Untargeted liposomes had no affinity for the dead and dying cell population.

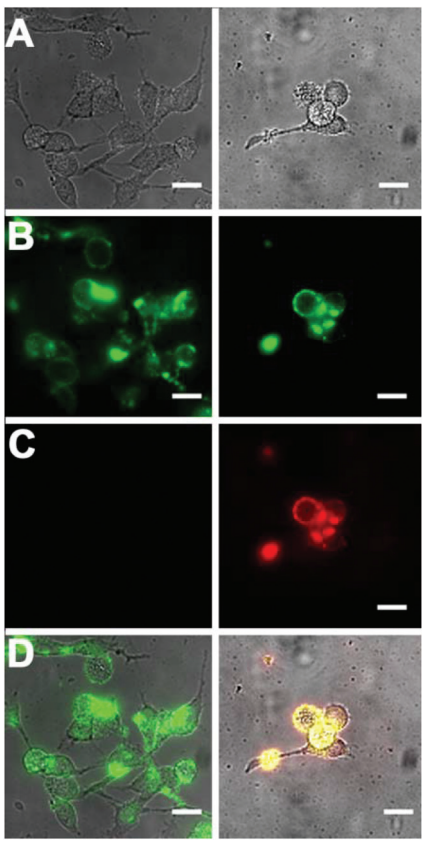

Fig. 6 Micrographs of human MDA-MB-211 cells treated with cytotoxic etoposide (10 μM) for 16 h and stained with green-emitting PSVue480 (10 μM), and either near-infrared fluorescent untargeted (left column) or Zn_2BDPA coated liposomes (right column). (row A) Brightfield; (row B) Green-emission from cells stained with PSVue480; (row C) Near-infrared emission from cells stained with liposomes; (row D) Overlay of A, B, and C. Scale bar = 30 μm.

Conclusion

The two amphiphilic conjugates, Zn_2BDPA-PEG_{2000}-DSPE and Zn_2BDPA-PEG_{500}-DSPE (Fig. 1C), were prepared using reliable synthetic methods and incorporated into liposomes at low molar fractions. Liposomes incorporating the shorter conjugate exhibited self-aggregation, whereas Zn_2BDPA coated liposomes incorporating the longer conjugate remained highly dispersed in aqueous solution. The Zn_2BDPA coated liposomes formed cross-linked precipitates with target liposomes containing anionic phospholipids, and did not interact with the liposomes composed of uncharged phospholipids that were mimics of the surfaces of healthy mammalian cells. The Zn_2BDPA coated liposomes selectively agglutinated bacterial cells in the presence of healthy human cells. The selective agglutination effect is most likely universal for both Gram-positive and Gram-negative bacteria since it targets the anionic amphiphiles in the bacterial envelope,[49] and is complementary to the highly specific cell recognition exhibited by antibodies which typically target a specific antigenic protein. The Zn_2BDPA affinity unit is not bactericidal but multivalent Zn_2BDPA coated liposomes may have value as immobilization agents that sequester an infection within an organism. Alternatively Zn_2BDPA coated liposomes may have potential as antibiotic delivery vehicles.[50,51] The selectivity for anionic cell surfaces was further demonstrated by selective staining of dead or dying mammalian cells in the presence of healthy cells, an experimental outcome that is consistent with the targeted liposome results of others.[52–54] While Zn_2BDPA coated liposomes could simply be employed as dead cell stains for *in vitro* assays, we envision a more ambitious *in vivo* application as a cell death "theranostic" platform that combines therapeutic and diagnostic capabilities within a single nanoparticle. Moreover, a liposomal system with both cell death targeting and cytotoxic delivery capability has the potential of producing amplified drug delivery to the dead and dying cells within cancerous tissue.[32,33]

Experimental

Materials

FmocNH-PEG_{500}-propionic acid (**8**) was obtained from Polypure (Oslo, Norway). H_2N-PEG_{2000}-DSPE, 1-palmitoyl-2-oleoyl-*sn*-glycero-3-phosphatidylcholine (POPC), 1-palmitoyl-2-oleoyl-*sn*-glycero-3-phosphatidylserine (POPS), 1,2-dipalmitoyl-*sn*-glycero-3-phosphatidylglycerol (DPPG), were obtained from Avanti Polar Lipids (Alabaster, Alabama, USA). The following fluorescent molecular probes were purchased and used as supplied PSVue480 (Molecular Targeting Technologies Inc.), DAPI and DiR (Life Technologies).

Synthesis

Proton (^{1}H-NMR) and carbon (^{13}C-NMR) nuclear resonance spectra were recorded on Varian UnityPlus 300 (300 MHz for ^{1}H, 75 MHz for ^{13}C), Varian INOVA 500 (500 MHz for ^{1}H, 125 MHz for ^{13}C), and Bruker Ascend 500 III HD (500 MHz for ^{1}H, 125 MHz for ^{13}C) NMR spectrometers. High resolution mass spectra were recorded on a Bruker micrOTOF II mass spectrometer using electrospray ionization (ESI). Analytical TLC was performed on EMD aluminum-backed 250 μm silica gel 60 F_{254} and on EMD aluminum-backed 250 μm neutral aluminum oxide 60 F_{254} plates. Analytical TLC visualization was done under UV light (254 nm) or using conventional staining methods (I_2, CAM, ninhydrin, sulfuric acid charring, and so on). Preparatory scale TLC (P-TLC) was done using SiliCycle glass-backed 1000 and 2000 μm silica gel 60 F_{254} plates. Flash column chromatography (FCC) was done by using either SiliCycle SiliaFlash P60 silica gel (40–63 μm, mesh 230–400) or Aldrich neutral aluminum oxide (Brockman I, 150 mesh, 58 Å). Anhydrous solvents for reactions were procured from commercial sources except for THF (purified using an Innovative Technologies SPS-100-2 solvent purification system) and $CHCl_3$ (distilled from P_2O_5).

(5-Hydroxy-1,3-phenylene)dimethanol (2). To a dispersion of 1 g (26.25 mmol) $LiAlH_4$ in 40 mL anhydrous THF at 0 °C was added drop-wise a solution of 3 g (14.27 mmol) dimethyl 5-hydroxyisophthalate. The reaction was allowed to heat to room temperature and stirred for 16 h. The reaction was cooled to 0 °C and 20 mL 10% (v/v) H_2SO_4 was added drop-wise. The solvent was removed under reduced pressure and residue was partitioned between 50 mL water and 50 mL EtOAc. The aqueous phase was saturated with NaCl. The aqueous phase was washed an additional 5 times using 50 mL EtOAc each. The combined organic layers were washed once with 100 mL saturated NaCl and dried with $MgSO_4$. The solvent was removed *in vacuo* to give 2.06 g (94% yield) of the desired material as a tan solid. R_f = 0.28 (SiO_2, EtOAc). ^{1}H NMR: (500 MHz, CD_3OD) δ 4.52 (s, 4H), 6.70 (s, 2H), 6.80 (s, 1H). ^{13}C NMR: (125 MHz, CD_3OD) δ 63.95, 112.49, 116.44, 143.13, 157.48. HRMS (ESI+) calculated for $C_8H_{10}O_3$ ($(M + H)^+$) 155.0703, found 155.0673

Ethyl 4-(3,5-bis(hydroxymethyl)phenoxy)butanoate (3). To a solution of 1 g (6.49 mmol) (5-hydroxy-1,3-phenylene)dimethanol, 3.80 g (19.46 mmol) ethyl 4-bromobutyrate, and 120 mg (0.32 mmol) tetrabutylammonium iodide in 15 mL anhydrous DMF was added 4.48 g (32.45 mmol) K_2CO_3. The reaction was stirred at 60 °C under Ar for 16 h. The solvent was removed under reduced pressure and the residue partitioned between 50 mL water and 50 ml EtOAc. The aqueous phase was washed an additional 2 times with 50 ml EtOAc each. The combined organic phases were washed with 100 mL saturated NaCl and dried with $MgSO_4$. Removal of the solvent and flash column chromatography (SiO_2, EtOAc) afforded 543 mg (~31% yield) of the desired compound as a pale yellow oil. R_f = 0.40 (SiO_2, EtOAc). ^{1}H NMR (300 MHz, $CDCl_3$) δ 1.26 (t, J = 7.18 Hz, 3H) 2.12 (m, 4H), 2.50 (t, J = 7.30 Hz, 2H), 4.01 (t, J = 6.10 Hz, 2H), 4.15 (q, J = 7.18 Hz, 2H), 4.64 (s, 4H) 6.82 (s, 2H) 6.91 (s, 1H). ^{13}C NMR (75 MHz, $CDCl_3$) δ 14.42, 24.79, 31.00, 60.80, 64.89, 66.94, 112.11, 117.74, 143.03, 159.25, 173.72. HRMS (ESI+) calculated for $C_{14}H_{20}NaO_5$ ($[M + H]^+$) 291.1206; found 291.1203.

Ethyl 4-(3,5-bis(bromomethyl)phenoxy)butanoate (4). To a solution of 170 mg (0.63 mmol) ethyl 4-(3,5-bis(hydroxymethyl)phenoxy)butanoate 415 mg (1.58 mmol) PPh_3, and 204 mg (1.58 mmol) DIPEA in 2 mL anhydrous THF was added drop-wise 524 mg (1.58 mmol) CBr_4 in 1 mL anhydrous THF. The reaction was allowed to proceed at r.t. under argon for 16 h. The reaction was quenched by addition of 10 mL saturated NaBr. The organic solvent was removed under reduced pressure. The residue was washed 3 times with 20 mL EtOAc. The combined organic phases were washed once with 30 mL saturated NaBr and dried using $MgSO_4$. The solvent was removed and the orange-brown residue subjected to flash column chromatography (SiO_2, 1 : 1 EtOAc–Hex) to give 241 mg (97% yield) of product as a pale yellow oil. R_f = 0.48 (SiO_2, 1 : 1 EtOAc–Hex). ^{1}H NMR (300 MHz, $CDCl_3$) δ 1.27 (t, J = 7.18 Hz, 3H), 2.12 (quin, J = 6.70 Hz, 2H), 2.53 (t, J = 7.29 Hz, 2H), 4.03 (t, J = 6.10 Hz, 2H), 4.16 (q, J = 7.18 Hz, 2H), 4.43 (s, 4H), 6.86 (d, J = 1.20 Hz, 2H), 7.00 (s, 1H). ^{13}C NMR (75 MHz, $CDCl_3$) δ 14.50, 24.77, 30.92, 33.13, 60.75, 67.13, 115.39, 122.10, 139.84, 159.46, 173.37. HRMS (ESI+) calculated for $C_{14}H_{18}Br_2O_3$ ($[M + H]^+$) 392.9695; found 392.9718.

Ethyl 4-(3,5-bis((bis(pyridin-2-ylmethyl)amino)methyl)-phenoxy)butanoate (5). To a solution of 680 mg (1.73 mmol) ethyl 4-(3,5-bis(bromomethyl)phenoxy)butanoate and 757 mg (3.80 mmol) picolylamine in anhydrous DMF was added 1.2 g (8.65 mmol) K_2CO_3. The reaction was stirred under Ar at r.t. for 16 h. The solvent was removed under vacuum and the residue partitioned between 20 mL each of water and $CHCl_3$. The aqueous phase was extracted 3 times using 20 mL $CHCl_3$. The combined organic phase was washed with 50 mL saturated NaCl, dried with $MgSO_4$, and the solvent was removed. The residue was subjected to flash column chromatography (Al_2O_3, $CHCl_3$–MeOH 98 : 2) and 1.05 g of product (96% yield) was obtained as a dark orange/brown oil. R_f = 0.77 (Al_2O_3, $CHCl_3$–MeOH 98 : 2). ^{1}H NMR (300 MHz, $CDCl_3$) δ 1.26 (t, J = 7.18 Hz, 3H), 2.11 (quin., J = 6.70 Hz, 2H) 2.53 (t, J = 6 Hz, 2H), 3.68 (s, 4H), 3.84 (s, 8H), 4.01 (t, J = 6.10 Hz, 2H), 4.15 (q, J = 7.18 Hz, 2H), 6.88 (s, 2H), 7.08 (s, 1H), 7.15 (ddd, J_1 = 6.76 Hz, J_2 = 4.96 Hz, J_3 = 1.91 Hz, 4H), 7.57–7.68 (m, 8H), 8.52 (d, J = 4.78 Hz, 4H). ^{13}C NMR (75 MHz, $CDCl_3$) δ 14.47, 24.92, 31.10, 58.75, 60.22, 60.65, 66.89, 113.75, 121.78, 122.23, 123.00, 136.69, 140.70, 149.17, 159.24, 159.78, 179.49. HRMS (ESI+) calculated for $C_{32}H_{42}N_6O_3$ ($[M + H]^+$) 631.3391, found 631.3423.

4-(3,5-Bis((bis(pyridin-2-ylmethyl)ammonio)methyl)phenoxy)-butanoate chloride (6). To a solution of 50 mg (77.5 μmol) ethyl 4-(3,5-bis((bis(pyridin-2-ylmethyl)amino)methyl)phenoxy)-butanoate in 2 mL THF–Water–MeOH (2 : 1 : 1) was added 60 μl (0.34 mmol) 20% (w/w) NaOH (aq.). The reaction was refluxed for 2 h, at which time TLC (Al_2O_3, $CHCl_3$–MeOH 98 : 2) indicated complete conversion of the starting material.

The pH of the reaction was adjusted to ~7 by addition of ~300 μl 1 M HCl. The solvents were removed under reduced pressure and the remaining solids were washed 3 times with 10 mL $CHCl_3$. The combined organic layers were dried with $MgSO_4$. Filtration and removal of solvent afforded ~50 mg (~99% yield) of the desired compound (BDPA-acid) as a pale yellow oil. R_f = 0.46 (Al_2O_3, $CHCl_3$–MeOH–H_2O 65 : 30 : 5); 0.27 (SiO_2, $CHCl_3$–MeOH–NH_4OH 8 : 2 : 0.2). ^{1}H NMR (500 MHz, CD_3OD) δ 2.05 (quin., 2H, J = 6.72 Hz), 2.47 (t, 2H, J = 7.21 Hz), 3.63 (s, 4H), 3.77 (s, 8H), 4.00 (t, J = 6.36 Hz, 2H), 6.83 (s, 2H), 6.99 (s, 1H), 7.21–7.28 (m, 4H), 7.64 (d, J = 7.83 Hz, 4H), 7.76 (td, J = 7.70 Hz, J = 1.71 Hz, 4H), 8.31–8.46 (m, 4H). ^{13}C NMR (125 MHz, CD_3OD) δ 24.80, 30.56, 58.69, 59.70, 66.94, 114.01, 121.77, 122.61, 123.54, 137.49, 140.16, 148.22, 159.22, 159.37, 176.07. HRMS (ESI+) calculated for $C_{36}H_{39}N_6O_3$ ($[M + H]^+$) 603.3078; found 603.3067.

BDPA-PEG$_{2000}$-DSPE (7). To a solution of 17.3 mg (0.027 mmol) BDPA-acid (**6**) and 5 mg pentafluorophenol (0.027 mmol) in 1.7 mL anhydrous $CHCl_3$ under argon at 0 °C was added drop wise 5.2 mg (0.027 mmol) EDC and 0.66 mg (0.0054 mmol) DMAP each in 0.1 mL anhydrous $CHCl_3$. The reaction was kept at 0 °C for 30 min and then allowed to warm to room temperature and stirred for 16 h. 30 mg (0.011 mmol) H_2N-PEG$_{2000}$-DSPE and 3.5 mg (4.7 μl, 0.011 mmol) DIPEA in 0.1 mL anhydrous $CHCl_3$ was added to the reaction and stirred at room temperature under argon for 24 h. The crude reaction mixture was subjected to preparatory scale TLC on silica using 8 : 2 : 0.2 $CHCl_3$–MeOH–NH_4OH as the eluent followed by a second P-TLC run on SiO_2 using 8 : 1 : 0.1 $CHCl_3$–MeOH–NH_4OH as the eluent to give 24 mg (~65% yield) of product as a yellow/orange solid film. R_f = 0.25 (SiO_2, 8 : 1 : 0.1 $CHCl_3$–MeOH–NH_4OH). ^{1}H NMR (300 MHz, $CDCl_3$, CD_3OD) δ 0.84 (t, J = 6 Hz, 6H), 1.21 (m, ~65H), 1.54 (m, 4H), 2.07 (m, 2H), 2.24 (td, J_1 = 7.53 Hz, J_2 = 2.39 Hz, 4H), 2.36 (m, 2H), 3.38 (m, 4H), 3.44–3.76 (m, ~216H), 3.85 (m, 10H), 3.95 (m, 6H), 4.07–4.22 (m, 4H), 4.34 (dd, J_1 = 12.08 Hz, J_2 = 3.23 Hz, 1H), 5.17 (m, 1H), 6.85 (s, 2H), 7.03 (s, 1H), 7.13–7.20 (m, 4H), 7.54–7.71 (m, 8H), 8.45 (d, J = 4.54 Hz, 4H). ^{13}C NMR (125 MHz, $CDCl_3$, CD_3OD) δ 14.25, 22.84, 25.04, 25.07, 25.50, 29.32, 29.51, 29.81, 29.86, 32.08, 32.87, 34.27, 34.44, 39.32, 42.41, 58.72, 59.69, 62.81, 63.57, 63.68, 64.42, 67.27, 69.89, 70.02, 70.23, 70.38, 70.63, 70.69, 114.18, 121.89, 122.55, 123.34, 137.23, 139.96, 148.77, 158.83, 159.39, 173.32, 173.72. HRMS (ESI+) calculated for $C_{168}H_{298}N_8O_{56}P^-$ ($[[M + 3H)/2]^+$) 1679.0339, found 1679.5384.

NH$_2$-PEG$_{500}$-DSPE (9). To a solution of 146 mg (0.174 mmol) **8** in 5 mL anhydrous $CHCl_3$ at 0 °C under argon was sequentially added 48 mg (0.261 mmol) pentafluorophenol, 50 mg (0.261 mmol) EDC, and 4.3 mg (34.8 μmol) DMAP. The reaction was kept at 0 °C for 30 min, then allowed to warm to room temperature and stirred for 16 h. To this reaction mixture was added 169 mg (0.226 mmol) DSPE followed by 33.7 mg (45.5 μl, 0.261 mmol) DIPEA in 1 mL anhydrous $CHCl_3$. The reaction was refluxed for 24 h after which the solvent was removed *in vacuo*. The residue was dissolved in minimal $CHCl_3$ and applied to a silica flash column and the product was eluted using 8 : 2 : 0.2 $CHCl_3$–MeOH–H_2O. Enriched fractions were pooled, the solvent was removed under reduced pressure, the residue was dissolved minimal $CHCl_3$, and was applied to a silica preparatory TLC plate which was developed using 8 : 2 : 0.2 $CHCl_3$–MeOH–H_2O to give 178 mg pure product. To remove ambiguity regarding the counterion 150 mg of product was dissolved in 50 mL $CHCl_3$ and washed 2 times with 50 mL saturated NaCl which was acidified to pH 4. The organic phase was dried using Na_2SO_4 and removal of solvent *in vacuo* yielded 146 mg (~65% yield) of FmocNH-PEG$_{500}$-DSPE. R_f = 0.46 (SiO_2, $CHCl_3$–MeOH–H_2O 8 : 2 : 0.2). ^{1}H NMR (300 MHz, $CDCl_3$) δ 0.88 (t, 3H), 1.19–1.39 (m, ~60H), 1.58 (m, 5H), 2.28 (td, J = 7.53, 2.63 Hz, 4H), 2.5 (t, J = 5.50 Hz, 2H), 3.26–3.50 (m, 5H), 3.50–3.82 (m, ~56H), 3.88 (t, J = 6.22 Hz, 1H), 4.00 (t, J = 5.86 Hz, 4H), 4.08–4.30 (m, 3H), 4.31–4.50 (m, 4H), 5.17–5.27 (m, 1H), 5.53 (m, 1H), 7.28–7.35 (m, 2H), 7.41 (t, J = 7.18 Hz, 2H), 7.61 (d, J = 7.41 Hz, 2H), 7.77 (d, J = 7.41 Hz). ^{13}C NMR (75 MHz, $CDCl_3$) δ 14.36, 15.34, 22.92, 25.08, 29.36, 29.59, 29.94, 32.14, 34.26, 34.41, 35.43, 36.56, 41.13, 42.76, 47.46, 62.41, 66.75, 67.43, 70.05, 70.26, 70.37, 70.75, 120.16, 125.28, 127.25, 127.86, 141.50, 144.19, 172.59, 173.20, 173.57, 173.62. HRMS (ESI+) calculated for $C_{83}H_{146}N_2O_{23}P^-$ ($(M + 2H)^+$) 1569.0054, found 1568.9970. 146 mg (91.8 μmol) of FmocNH-PEG$_{500}$-DSPE was dissolved in 5 mL 20% piperidine in DMF. The reaction was allowed to proceed for 2 h at room temperature, after which the solvent was removed *in vacuo* and the residue was subjected to flash column chromatography (SiO_2, $CHCl_3$–MeOH–water 8 : 2 : 0.2) 4 times to yield enriched product. This material was purified after two runs on preparatory TLC (SiO_2, $CHCl_3$–MeOH–H_2O 8 : 2 : 0.2). 90 mg (~73% yield) of product was obtained as a white solid. R_f = 0.26 (SiO_2, $CHCl_3$–MeOH–H_2O 8 : 2 : 0.2). ^{1}H NMR (300 MHz, $CDCl_3$) δ 0.88 (t, 6H), 1.26 (m, ~58H), 1.59 (m, 4H), 2.29 (td, J = 7.59, 3.95 Hz, 5H), 2.50 (t, J = 6.10 Hz, 2H), 3.19 (m, 2H), 3.38–3.52 (m, 3H), 3.53–3.86 (m, ~51H), 3.94–4.09 (m, 2H), 4.17 (dd, J = 12.08, 6.58 Hz, 1H), 4.40 (dd, J = 11.96, 3.35, 1H), 5.22 (m, 1H). ^{13}C NMR (75 MHz, $CDCl_3$) δ 13.69, 22.51, 24.74, 24.77, 29.00, 29.18, 29.22, 29.51, 29.55, 31.79, 33.91, 34.04, 36.29, 39.42, 62.18, 64.18, 64.88, 66.64, 66.99, 69.52, 69.66, 69.73, 69.83, 69.90, 69.97, 70.09, 70.17, 70.23, 173.35, 173.75. HRMS (ESI+) calculated for $C_{68}H_{134}N_2O_{21}P^-$ ($(M + 2H)^+$) 1347.9368, found 1347.9354; MS (ESI+) calculated for $C_{68}H_{134}N_2O_{21}P^-$ ($(M + H + Na)^+$) 1369.9187, found 1369.9177.

BDPA-PEG$_{500}$-DSPE (10). To a solution of 88.9 mg (0.139 mmol) BDPA-acid (**6**) and 25.6 mg pentafluorophenol (0.139 mmol) in 3 mL anhydrous $CHCl_3$ under argon at 0 °C was added drop wise 26.6 mg (0.139 mmol) EDC and 3.33 mg (0.0273 mmol) DMAP each in 0.5 mL anhydrous $CHCl_3$. The reaction was kept at 0 °C for 30 min and then allowed to warm to room temperature and stirred for 16 h. 80 mg (0.0594 mmol) H_2N-PEG$_{500}$-DSPE and 19.2 mg (25.9 μl, 0.149 mmol) DIPEA in 0.5 mL anhydrous $CHCl_3$ was added to the reaction and stirred at room temperature under argon for 24 h. The crude reaction mixture was subjected to preparatory scale TLC on silica using 8 : 2 : 0.2 $CHCl_3$–MeOH–NH_4OH as

the eluent followed by a second P-TLC run on SiO_2 using 8 : 1 : 0.1 $CHCl_3$–MeOH–NH_4OH as the eluent to give 100 mg (~86% yield) of product as an orange/brown solid film. R_f = 0.50 (SiO_2, 8 : 2 : 0.2 $CHCl_3$–MeOH–NH_4OH). ^{1}H NMR (300 MHz, $CDCl_3$) δ 0.87 (t, J = 6 Hz, 6H), 1.25 (m, 60H), 1.57 (m, 4H), 2.11 (m, 2H), 2.27 (m, 4H), 2.41 (t, J = 6 Hz, 2H), 2.48 (t, J = 6 Hz, 2H), 3.45 (m, 4H), 3.50–3.79 (m, 59H), 3.86 (s, 8H), 3.99 (m, 6H), 4.17 (dd, J_1 = 11.96 Hz, J_2 = 6.70 Hz, 1H), 4.39 (dd, J_1 = 12.20 Hz, J_2 = 3.11 Hz, 1H), 5.23 (m, 1H), 6.88 (s, 2H), 7.06 (s, 1H), 7.17 (m, 4H), 7.58–7.71 (m, 8H), 8.53 (d, J = 5.02 Hz, 4H). ^{13}C NMR (75 MHz, $CDCl_3$) δ 14.10, 22.66, 24.85, 24.89, 25.28, 29.11, 29.30, 29.33, 29.63, 29.68, 31.89, 32.76, 34.07, 34.25, 36.74, 39.15, 58.48, 59.50, 62.65, 66.98, 67.45, 69.84, 70.07, 70.10, 70.43, 113.72, 122.11, 122.95, 136.11, 148.72, 159.07, 171.36, 172.48, 172.99, 173.37. HRMS (ESI−) calculated for $C_{104}H_{170}N_8O_{23}P^-$ (M^-) 1931.2155, found 1931.2042.

Liposome studies

Liposome preparation for cuvette experiments. All polar lipids were purchased from Avanti Polar lipids (Alabaster, AL, USA) and were used without further purification. Lipid films consisting of appropriate molar fractions of polar lipid (3.32 μmol total lipid) were prepared by dispensing measured aliquots from stock chloroform solutions, evaporating the solvent under a gentle stream of argon, and placing the films under vacuum overnight to ensure complete removal of solvent. The films were hydrated by adding 1 mL of HEPES buffer (pH 7.4, 10 mM HEPES, 137 mM NaCl, 3.2 mM KCl, 2 mM NaN_3) or in some cases a 1 mL solution of HEPES buffer containing $Zn(NO_3)_2$. The hydrated lipid films were subjected to six freeze–thaw cycles (40 °C ↔ liquid N_2) and then passed 21 times through a 19 mm polycarbonate Nucleopore filter with 200 nm diameter pores using an Avestin LiposoFast mini extruder to produce unilamellar liposomes. Aliquots (125 μL) of Zn_2BDPA coated liposomes were diluted by adding HEPES buffer (875 μL) and subjected to dynamic light scattering (DLS) analysis using a Zetasizer Nano ZS particle sizer (25 °C, 173.1° backscatter angle with appropriate material, dispersant, and RI parameters selected). Liposome cross-linking experiments mixed 500 μL of HEPES buffer with 250 μL of liposomes composed of Zn_2BDPA-PEG_{2000}-DSPE–cholesterol–POPC (2.5 : 30 : 67.5) and 250 μL of target liposomes with various compositions. The results were photographed using a digital camera.

Fluorescent liposome preparation for cell studies. Liposomes containing 2 mol% 1,1′-dioctadecyl-3,3,3′,3′-tetramethylindotricarbocyanine iodide (DiR) were prepared using the thin film hydration method described above, and a zinc-containing hydration buffer (10 mM HEPES, 145 mM NaCl, 100 μM $ZnNO_3$, pH = 7.4).

Bacterial agglutination studies. Samples of *Staphylococcus aureus* NRS11 (gift from Professor S. Mobashery), *Escherichia coli* UTI89 (gift from Professor D. Piwnica-Worms), *Klebsiella pneumoniae* (ATCC #33495), and *Pseudomonas aeruginosa* (containing mini-Tn7 chromosomal, constitutive, GFP-expressing insertions, gift from Professor J. Shrout) were grown to mid-log phase (OD = 0.5) in Luria Bertani (LB) broth (5 g L^{-1} yeast extract, 10 g L^{-1} Tryptone, 10 g L^{-1} NaCl) at 37 °C and a shaker speed of 200 rpm. The samples were centrifuged (5000 rpm, 5 min) and the pellet resuspended in 1 mL of HEPES buffer (10 mM HEPES, 145 mM NaCl, pH = 7.4). Each sample of bacteria (~10^8 cells) was treated for 15 min with near-infrared fluorescent Zn_2BDPA coated liposomes (Zn_2BDPA-PEG_{2000}-DSPE–DiR–cholesterol–POPC, 2 : 2 : 30 : 66) or untargeted liposomes (DiR–cholesterol–POPC, 2 : 30 : 68). The treated cells were pelleted by microcentrifugation at 5000 rpm for 5 min and the tubes were imaged using a CCD camera within a Xenogen imaging station. A region of interest analysis of the fluorescence images indicated that the pellets contained 98% and 6% of the Zn_2BDPA coated liposomes and untargeted liposomes, respectively. The bacterial cells were washed twice with buffer to reduce background fluorescence, dispersed into solution then onto slides, and micrographs were acquired using a Nikon Eclipse TE2000-U epifluorescence microscope with a 60× objective and a Photometrics Cascade 512B CCD. Near infrared fluorescence images were captured using a Cy7 filter set (Exciter HQ710/75x, Dichroic Q750LP, Emitter HQ810/90m).

Fluorescence microscopy was used to demonstrate the selectivity of the Zn_2BDPA coated liposomes for bacterial cells over healthy mammalian cells. The nuclei of confluent MDA-MB-231 human breast cancer cells were stained by incubating with DAPI (1 μg mL^{-1} DAPI in PBS) for 30 minutes. Separate samples of the DAPI stained MDA-MB-231 cells were washed with HEPES buffer then treated with near-infrared fluorescent Zn_2BDPA coated liposomes or untargeted liposomes in HEPES buffer. An aliquot of GFP-expressing *P. aeruginosa* (20 μL from a broth grown to an OD_{600} = 0.2) was added to the samples, which were incubated for 15 minutes then imaged using fluorescence microscopy. Fluorescence images were captured using UV (ex: 340/80, em: 435/85), GFP (ex: 450/90, em: 500/50), or Cy7 filter sets.

Mammalian cell toxicity

Toxicity of the liposomal formulations was measured using the 3-(4,5-dimethylthiazol-2-yl)-2,5 diphenyltetrazolium bromide (MTT) cell vitality assay. MDA-MB-231 human breast cancer cells (ATCC) were seeded into 96-microwell plates, and grown to a confluency of 85% in RPMI media with 10% fetal bovine serum, and 1% streptavidin L-glutamate at 37 °C and 5% CO_2. The Vybrant MTT Cell Proliferation Assay Kit (Invitrogen, Eugene, USA) was performed according to the manufacturer's protocol and validated using 10 μM etoposide as a positive control for high toxicity. The cells were treated with untargeted liposomes (cholesterol–POPC, 30 : 70) and Zn_2BDPA coated liposomes (Zn_2BDPA-PEG_{2000}-DSPE–cholesterol–POPC, 2 : 30 : 68) and incubated for 18 h at 37 °C. The medium was removed and replaced with 100 μL of RPMI media containing MTT (1.2 mM). An SDS detergent solution was added and incubated at 37 °C and 5% CO_2 for an additional 4 hours. The absorbance of each well was read at 570 nm and the normalized

data (measured in triplicate) are shown in Fig. ESI-7.† The results indicate that the untargeted and Zn_2BDPA coated liposomes induce negligible amounts of cell death at concentrations <10 μM and <25 μM respectively.

Mammalian cell death imaging using fluorescent liposomes

Confluent MDA-MB-211 cells were treated with etoposide (10 μM) for 16 hours to induce apoptotic cell death. Separate populations of apoptotic MDA cells were treated with near-infrared fluorescent Zn_2BDPA coated liposomes or untargeted liposomes in HEPES buffer and allowed to incubate for 15 minutes. The cells were then washed three times followed by treatment with green-emitting cell death probe PSVue480 (10 μM) for 15 minutes and three subsequent wash steps. Fluorescence micrographs were captured using the microscope described above and a GFP or Cy7 filter set.

Acknowledgements

This study was supported by the NIH (RO1GM059078 to B.D.S. and T32GM075762 to D.R.R.), Walther Cancer Research Foundation, the University of Notre Dame, the Notre Dame Integrated Imaging Facility, and the Freimann Life Sciences Center. S.T. gratefully acknowledges support from the Scientific and Technological Research Council of Turkey (Grant number 114C041).

Notes and references

1 T. Sakamoto, A. Ojida and I. Hamachi, *Chem. Commun.*, 2009, 141–152.
2 M. Kruppa and B. Konig, *Chem. Rev.*, 2006, **106**, 3520–3560.
3 E. J. O'Neil and B. D. Smith, *Coord. Chem. Rev.*, 2006, **250**, 3068–3080.
4 S. K. Kim, D. H. Lee, J.-I. Hong and J. Yoon, *Acc. Chem. Res.*, 2008, **42**, 23–31.
5 Y. Zhou, Z. Xu and J. Yoon, *Chem. Soc. Rev.*, 2011, **40**, 2222–2235.
6 H. T. Ngo, X. Liu and K. A. Jolliffe, *Chem. Soc. Rev.*, 2012, **41**, 4928–4965.
7 M. S. Han and D. H. Kim, *Angew. Chem., Int. Ed.*, 2002, **41**, 3809–3811.
8 D. H. Lee, J. H. Im, S. U. Son, Y. K. Chung and J. I. Hong, *J. Am. Chem. Soc.*, 2003, **125**, 7752–7753.
9 D. H. Lee, S. Y. Kim and J. I. Hong, *Angew. Chem., Int. Ed.*, 2004, **43**, 4777–4780.
10 J. H. Lee, J. Park, M. S. Lah, A. Chin and J. I. Hong, *Org. Lett.*, 2007, **9**, 3729–3731.
11 S. W. Bae, M. S. Cho, A. R. Jeong, B. R. Choi, D. E. Kim, W. S. Yeo and J. I. Hong, *Small*, 2010, **6**, 1499–1503.
12 D. J. Oh, K. M. Kim and K. H. Ahn, *Chem. – Asian J.*, 2011, **6**, 2033–2038.
13 G. Liu, K. Y. Choi, A. Bhirde, M. Swierczewska, J. Yin, S. W. Lee, J. H. Park, J. I. Hong, J. Xie, G. Niu, D. O. Kiesewetter, S. Lee and X. Chen, *Angew. Chem., Int. Ed.*, 2012, **51**, 445–449.
14 K. Honda, S. H. Fujishima, A. Ojida and I. Hamachi, *ChemBioChem*, 2007, **8**, 1370–1372.
15 A. Ojida, K. Honda, D. Shinmi, S. Kiyonaka, Y. Mori and I. Hamachi, *J. Am. Chem. Soc.*, 2006, **128**, 10452–10459.
16 K. Honda, E. Nakata, A. Ojida and I. Hamachi, *Chem. Commun.*, 2006, 4024–4026.
17 J. A. Drewry, S. Burger, A. Mazouchi, E. Duodu, P. Ayers, C. C. Gradinaru and P. T. Gunning, *MedChemComm*, 2012, **3**, 763–770.
18 J. R. Morrow and O. Iranzo, *Curr. Opin. Chem. Biol.*, 2004, **8**, 192–200.
19 V. Ganesh, K. Bodewits, S. J. Bartholdson, D. Natale, D. J. Campopiano and J. C. Mareque-Rivas, *Angew. Chem., Int. Ed.*, 2009, **48**, 356–360.
20 E. Kinoshita, M. Takahashi, H. Takeda, M. Shiro and T. Koike, *Dalton Trans.*, 2004, 1189–1193, DOI: 10.1039/b400269e.
21 L. Ciavatta, J. C. Mareque, D. Natale and F. Salvatore, *Ann. Chim.*, 2006, **96**, 317–325.
22 A. V. Koulov, K. A. Stucker, C. Lakshmi, J. P. Robinson and B. D. Smith, *Cell Death Differ.*, 2003, **10**, 1357–1359.
23 A. V. Koulov, R. G. Hanshaw, K. A. Stucker, C. Lakshmi and B. D. Smith, *Isr. J. Chem.*, 2005, **45**, 373–379.
24 R. G. Hanshaw, C. Lakshmi, T. N. Lambert, J. R. Johnson and B. D. Smith, *ChemBioChem*, 2005, **6**, 2214–2220.
25 W. M. Leevy, S. T. Gammon, J. R. Johnson, A. J. Lampkins, H. Jiang, M. Marquez, D. Piwnica-Worms, M. A. Suckow and B. D. Smith, *Bioconjugate Chem.*, 2008, **19**, 686–692.
26 B. A. Smith, W. J. Akers, W. M. Leevy, A. J. Lampkins, S. Xiao, W. Wolter, M. A. Suckow, S. Achilefu and B. D. Smith, *J. Am. Chem. Soc.*, 2010, **132**, 67–69.
27 B. A. Smith, S. Xiao, W. Wolter, J. Wheeler, M. A. Suckow and B. D. Smith, *Apoptosis*, 2011, **16**, 722–731.
28 B. A. Smith, B. W. Xie, E. R. van Beek, I. Que, V. Blankevoort, S. Xiao, E. L. Cole, M. Hoehn, E. L. Kaijzel, C. W. Lowik and B. D. Smith, *ACS Chem. Neurosci.*, 2012, **3**, 530–537.
29 S. Xiao, S. Turkyilmaz and B. D. Smith, *Tetrahedron Lett.*, 2013, **54**, 861–864.
30 S. Xiao, L. Abu-Esba, S. Turkyilmaz, A. G. White and B. D. Smith, *Theranostics*, 2013, **3**, 658–666.
31 B. A. Smith, K. M. Harmatys, S. Xiao, E. L. Cole, A. J. Plaunt, W. Wolter, M. A. Suckow and B. D. Smith, *Mol. Pharmaceutics*, 2013, **10**, 3296–3303.
32 X. He, N. Bonaparte, S. Kim, B. Acharya, J. Y. Lee, L. Chi, H. J. Lee, Y. K. Paik, P. G. Moon, M. C. Baek, E. K. Lee, J. H. Kim, I. S. Kim and B. H. Lee, *J. Controlled Release*, 2012, **162**, 521–528.
33 K. Wang, M. H. Na, A. S. Hoffman, G. Shim, S. E. Han, Y. K. Oh, I. C. Kwon, I. S. Kim and B. H. Lee, *J. Controlled Release*, 2011, **154**, 214–217.
34 Y. Barenholz, *J. Controlled Release*, 2012, **160**, 117–134.
35 H. Maeda, *Bioconjugate Chem.*, 2010, **21**, 797–802.

36 E. A. Azzopardi, E. L. Ferguson and D. W. Thomas, *J. Antimicrob. Chemother.*, 2013, **68**, 257–274.
37 Y. H. Bae and K. Park, *J. Controlled Release*, 2011, **153**, 198–205.
38 Z. Cheng, A. Al Zaki, J. Z. Hui, V. R. Muzykantov and A. Tsourkas, *Science*, 2012, **338**, 903–910.
39 P. Ruenraroengsak, J. M. Cook and A. T. Florence, *J. Controlled Release*, 2010, **141**, 265–276.
40 N. Bertrand and J. C. Leroux, *J. Controlled Release*, 2012, **161**, 152–163.
41 I. K. Kwon, S. C. Lee, B. Han and K. Park, *J. Controlled Release*, 2012, **164**, 108–114.
42 S. M. Moghimi, A. C. Hunter and T. L. Andresen, *Annu. Rev. Pharmacol. Toxicol.*, 2012, **52**, 481–503.
43 C. Lakshmi, R. G. Hanshaw and B. D. Smith, *Tetrahedron*, 2004, **60**, 11307–11315.
44 P. R. Ashton, D. W. Anderson, C. L. Brown, A. N. Shipway, J. F. Stoddart and M. S. Tolley, *Chem. – Eur. J.*, 1998, **4**, 781–795.
45 R. Appel, *Angew. Chem., Int. Ed.*, 1975, **14**, 801–811.
46 E. Valeur and M. Bradley, *Chem. Soc. Rev.*, 2009, **38**, 606–631.
47 A. Samad, Y. Sultana and M. Aqil, *Curr. Drug Delivery*, 2007, **4**, 297–305.
48 J. J. Lee, K. J. Jeong, M. Hashimoto, A. H. Kwon, A. Rwei, S. A. Shankarappa, J. H. Tsui and D. S. Kohane, *Nano Lett.*, 2014, **14**, 1–5.
49 C. Ratledge and S. G. Wilkinson, *Microbial Lipids*, Academic Press, London, 1988.
50 C. M. Huang, C. H. Chen, D. Pornpattananangkul, L. Zhang, M. Chan, M. F. Hsieh and L. F. Zhang, *Biomaterials*, 2011, **32**, 214–221.
51 K. W. Yang, B. Gitter, R. Ruger, G. D. Wieland, M. Chen, X. L. Liu, V. Albrecht and A. Fahr, *Photochem. Photobiol. Sci.*, 2011, **10**, 1593–1601.
52 Y. S. Cho, K. M. Kim, D. Lee, W. J. Kim and K. H. Ahn, *Chem. – Asian. J.*, 2013, **8**, 755–759.
53 B. Garnier, A. Bouter, C. Gounou, K. G. Petry and A. R. Brisson, *Bioconjugate Chem.*, 2009, **20**, 2114–2122.
54 For a general review regarding liposomes coated with metal complexes, including those with targeting capability, see: B. Gruber and B. Konig, *Chem. – Eur. J.*, 2013, **19**, 438–448.